Published in final edited form as:
Anal Chem. 2010 March 1; 82(5): 1634–1642. doi:10.1021/ac901955d.

Approaches to Increasing Surface Stress for Improving Signal-to-Noise Ratio of Microcantilever Sensors

Hai-Feng Ji* and **Benjamin D. Armon**
Department of Chemistry, Drexel University, Philadelphia, PA 19010

Summary

Microcantilever sensor technology has been steadily growing for the last fifteen years. While we have gained a great amount of knowledge in microcantilever bending due to surface stress changes, which is a unique property of microcantilever sensors, we are still in the early stages of understanding the fundamental surface chemistries of surface-stress-based microcantilever sensors. In general, increasing surface stress, which is caused by interactions on the microcantilever surfaces, would improve the S/N ratio, and subsequently the sensitivity and reliability of microcantilever sensors. In this review, we will summarize: A) the conditions under which a large surface stress can readily be attained, and B) the strategies to increase surface stress in case a large surface stress can not readily be reached. We will also discuss our perspectives on microcantilever sensors based on surface stress changes.

1. Introduction

Advances in the field of micro-electro-mechanical systems (MEMS) and their uses offer unique opportunities for the design of small-size and cost-effective analytical methods. In 1994, it was realized that microcantilevers could be made extremely sensitive to chemical and physical changes.[1,2,3] Several electron micrographs of microcantilevers are shown in Figure 1. To date, physical sensing has been demonstrated through detection of thermal energy,[3, 4] radiation, [5] strain, [6] magnetic fields, [7] electric charge, [8] viscosity,[9] density,[10] molecular beams,[11] and infrared.[12] Extremely sensitive chemical and biological sensors based on microcantilevers, including those for DNA,[13,14] alcohol,[15] mercury, [16] antigen, [17] etc. have been demonstrated using selective coatings on the cantilever.

Two characteristics of a microcantilever, resonance frequency and bending, can be used to detect chemicals. We focus on the bending of microcantilevers in this review. Microcantilevers undergo bending due to molecular interactions by confining the interactions to one side of the cantilever. Adsorption or intercalation of the analyte will change the surface characteristics of the microcantilever or the film volume on the cantilever, and results in the bending of the microcantilever. Using Stoney's formula,[18] the radius of curvature of bending of the cantilever due to adsorption can be written as:

$$\Delta z = \left(\frac{3(1-\upsilon)l^2}{Et^2}\right)\delta s, \tag{1}$$

* Corresponding author: hj56@drexel.edu, Phone: 01-215-895-2562, Fax: 01-215-895-1605.

where Δz is the observed deflection at the end of the cantilever, ν and *E* are Poisson's ratio (0.2152) and Young's modulus (156 GPa for silicon) for the substrate, respectively. *t* and *l* are the thickness and length of the cantilevers, respectively, and *δs* is the differential stress on the cantilever.

When layer of the molecules receptor is thin, such as a monolayer, it can be neglected. However, when the substrate of the cantilever is made of bilayered materials and neither of the layers can be neglected, then the equation is expressed as: [19]

$$\Delta z = \frac{3l}{t_1+t_2}\left[\frac{1+(\frac{t_1}{t_2})^2}{3(1+\frac{t_1}{t_2})^2+(1+\frac{t_1E_1}{t_2E_2})(\frac{t_1^2}{t_2^2}+\frac{t_2E_2}{t_1E_1})}\right]\times\frac{\Delta s}{E*}, \quad (2)$$

where t_1 and t_2 are the thickness of the two layers of the microcantilever substrate, E_1 and E_2 are Young's moduli for the coating and microcantilever, respectively, and E^* is the effective Young's modulus for the coated microcantilever, with $E^*=E_1E_2/(E_1+E_2)$, Δs is the differential stress on the cantilever.

Microcantilevers can bend up or down upon binding of specific species in the environment depending on different effects as shown in Figure 2. By monitoring changes in the bending response of a cantilever, surface stress changes induced by either adsorption or molecular recognition can be accurately recorded. Optical,[1] piezoresistive,[20] piezoelectric,[12] and capacitive[21] methods have been used for detection of cantilever deflection.

The bending of microcantilevers has been demonstrated to detect chemicals with sensitivities as high as parts-per-trillion (ppt) to parts-per-quadrillion (ppq).[22] Compared to traditional technologies for the detection of chemicals, the microcantilever sensor has three key advantages: high sensitivity at a low cost, low-power consumption, and a small size. These characteristics make the microcantilever a reasonably good sensor platform for either on-site chemical verification or medical diagnostics.

One challenge to many surface-stress-based microcantilever sensors is their low signal/noise (S/N) ratios. Although a surface stress less than 0.0001 N/m can be reached, variations in temperature and any slight variation of the electrolyte concentration can produce significant surface stress between 0.002-0.005 N/m. If the S/N ratio is small, it requires hours to reach a good baseline (< 0.001 N/m surface stress because of noises) before each test. The small S/N ratio and the long waiting time are the main obstacles towards commercializing microcantilever technology. In some cases, the S/N ratios are too small to detect the targeted analyte, even when the analyte concentration is high.

A significant amount of effort has been focused on the optimization of microcantilever structures to reduce noise, which has been reviewed elsewhere.[23] While this is essential for developing low-cost and practical microcantilever instrumentation, the optimization of the surface chemistry of receptors on the microcantilever surface is equally important. One possibility for optimization of surface chemistry for microcantilever sensors is to increase the surface stress and thus the bending amplitude of microcantilevers, on analyte-receptor interaction. The optimized conjugation chemistry specifically tailored to microcantilever sensors will create sensors with improved response characteristics.

In this review, we will summarize approaches that enhance surface stress for optimizing the sensing responses. This paper is organized with two sections:

Section A. Under those conditions in which a large surface stress (greater than 0.1 N/m) can readily be reached.

Section B. The strategies to increase surface stress for those conditions under which a large surface stress can not readily be reached.

Firstly, though, it is important to note:

1. It should be mentioned that although increasing surface stress and the S/N ratio would increase the bending amplitude and subsequently the sensitivity, the detection limit of these sensors is mainly determined by the binding constant of the analytes with the receptors on the surface. For this reason, the detection limits of the sensors will not be discussed. In this review, we will only discuss those microcantilever sensors with surface stresses that are greater than 0.1 N/m. We chose this number because user-friendly devices based on microcantilever sensors can be readily fabricated when the surface stress is greater than 0.1 N/m, based on the observation that a 0.01 N/m noise level baseline can be achieved in seconds. According to analytical chemistry terms, a signal/noise ratio of 3 is regarded as the detection limit.

2. Surface stress is proportional to the concentration of analytes adsorbed/absorbed on the cantilever surface. Proper analysis of various surface chemistries requires comparison of the surface stresses when the analyte-receptor interactions are saturated. However, for various reasons, most of the reviewed publications either did not or could not show the maximum surface stresses at saturation. Because of this, the cited maximum surface stresses in this review from papers on different systems could not be used to draw conclusions on the performance of the surface chemistries for comparison. It did, however, provide information for a quantitative analysis of the surface chemistries to a certain extent.

3. Most groups only reported bending amplitudes of the microcantilevers rather than the surface stresses. These bending amplitudes were measured from microcantilevers of different sizes and compositions. For comparison, we converted all the bending amplitude data to surface stresses according to Equations 1 and 2. For consistency, the following parameters have been used in all of the calculations: Poisson's ratio $\nu = 0.2152$ and Young's modulus E =156 GPa for silicon, 70 GPa for SiO_2, and 300 GPa for Si_3N_4. A 0.1 N/m surface stress corresponds to 60 nm of bending of a Si cantilever with the dimensions of 200 μm in length and 1 μm in thickness. It should be noted that surface stress is a general term used to elucidate the cause of microcantilever bending. In general, surface stress is a result of intermolecular interactions on the surface (such as electrostatic repulsion and/or attraction, steric effects, or hydration), changes in the volume of the coating, or thermal expansion differences between the two surfaces of the microcantilevers. When the coating is thicker, the film stress should be expressed with the same units as pressure (N/m^2). [24,25] To avoid confusion, we will not show the quantities for the surface stress change when a thicker coating was used, but simply address that the bending amplitude was large. This is based on the fact that the bending amplitude is our concern and that the bending amplitudes of all the thicker-film-coated microcantilevers were large. It should also be noted that some publications were not cited in this review because it is not possible to convert the only reported signals, which were in units of voltage, to surface stress without further information.

Section A. Under those conditions in which a large surface stress (greater than 0.1 N/m) can readily be reached

A1. Surface stress caused by chemical reactions

Chemical reactions can normally cause significant surface stress due to heat release or through the formation of different chemical species on the cantilever surfaces.

A1.1. Catalyst on microcantilever surfaces for reactions with a heat release— For this method, microcantilevers function as bimetallic thermal sensors and the heat released from the reaction will bend the microcantilevers. In general, chemical reactions on the catalytic surface produce enough heat to generate a large surface stress, such as a 4.5 N/m surface stress as a result of the reaction $H_2 + O_2 \rightarrow H_2O$[1], and a 1.5 N/m surface stress change from the oxidation of ethanol on a TiO_2 surface.[26] A significant difference in thermal expansion between the two layers (such as Si and Al) of the microcantilevers is critical for a larger surface stress change.[1, 27] The surface stress caused by catalytic reactions can be enhanced with optimized microcantilever structures and thermal expansion materials, such as a polymer-metal-ceramic trilayer. [28]

A1.2. Polymerization on the surface—Polymerization changes the volume and the internal tension of the film on the surface, which generates a substantial surface stress on the microcantilever. As an example,[5] the polymerization of Norland 61, a photocurable adhesive, with UV light generated more than 1.1 N/m of surface stress.

A1.3. Change of surface characteristics due to formation of new chemical species—The formation of an amalgam, made by the combination of mercury or mercury ions with the gold layer on the microcantilever, produces a surface stress that is greater than 1.0 N/m, which is useful for the sensitive detection of mercury and mercury ions. [29,30,31] Other examples include the interaction of Ca^{2+} with OH^- and NH_2 species on the Si_3N_4 surface (0.46 N/m of surface stress), [32] the conversion of SiOH to SiO^- or $SiOH^+$,[33] an interaction of the surface charges with Na^+ ions in a salt solution,[34] hydrogen bonding between water vapor and 4-mercaptobenzoic acid (3.2 N/m of surface stress),[35] the interaction of the same coating with trinitrobenzene (0.76 N/m of surface stress), and the of $HS(CH_2)_2COOH$ with protons or OH^- (3.0 N/m of surface stress).[36]

A1.4. Electrochemical reactions—Electrochemical reactions on microcantilevers (Figure 3) represent one family in the growing field of chemical detections. The surface stresses due to electrochemical reactions were in general greater than 0.1 N/m (Table 1)

As one example, the large stress change observed for the oxidation of ferrocenylundecanethiolate (FcC11SAu) modified microcantilever was attributed to steric constraints in the closely-packed FcC11SAu monolayer and the efficient coupling between the adsorbed FcC11S-monolayer and the Au-coated microcantilever transducer. The cantilever responds to the lateral pressure exerted by an ensemble of reorienting ferrocenium-bearing alkylthiolates stacked upon each other. This finding suggests that the cantilever responds to collective in-plane molecular interactions rather than to individual biochemical events. Large bending amplitudes were also observed on electrochemical deposition of a polyaniline film[43] and redox reaction of a Polypyrrole (PPy) film.[44]

A2. Surface stress created by changing the volume of polymer coatings

Polymers are among the first materials used to modify microcantilevers for sensing applications. The shrink or swell of the polymers generally causes a surfaces stress change that is usually greater than 0.1 N/m. There are several forces involved in film swelling, including

steric, electrostatic, hydration forces, etc. The sensitivity and selectivity of the sensor is mainly determined by the properties of the polymers. Some polymers selectively absorb more target analytes than others.[45,46] Most of the reports showed that microcantilevers coated with thicker polymer films generated more bending on their interaction with analytes. Several approaches have been applied to deposit polymers on the microcantilever surface.

A2.1 Spray coating, spin coating, and drop-casting—For these methods, polymers were first dissolved in solvents and then transferred to a microcantilever surface using the appropriate tools. A uniform polymer film forms on the microcantilever surface after solvent evaporation. Table 2 shows several polymers that have been coated on a microcantilever for chemical detection. Upon analyte absorption, all of these polymer-based cantilevers had large bending amplitudes corresponding to surface stresses that are greater than 0.1 N/m.

Protein films also function similarly to polymer films and large surface stress changes were observed when the analytes bound onto these protein films. As an example, microcantilevers modified by a layer of AgNt84-6, a metal binding protein, have been developed for the detection of a group of metal ions.[54]

A2.2 Crosslinked on the surface directly—This method is used to prepare crosslinked polymers on microcantilever surfaces since the crosslinked polymers can not be dissolved in any solvents. These polymers, such as crosslinked polystyrene, [55] poly(methacrylic acid)-poly (ethylene glycol) dimethacrylate hydrogels,[56,57, 58, 59] chitosan hydrogels,[60] and elastin-like polypeptides,[61] can be formed on the surface directly from their precursors.

A2.3 Layer-by-Layer (LbL) Assembly—This is one of the newer approaches for modifying microcantilever surfaces. The surface of the cantilever is modified through a positive and negative charge distribution technique. Microcantilevers that are modified with polyelectrolyte multilayers generate more surface stress than the corresponding monolayer films. One example is a cantilever modified by three-bilayers of glucose oxidase / polyethyleneimine (Figure 4) compared to a microcantilever that is modified by only one layer of glucose oxidase. The first cantilever has a 0.08 N/m surface stress,[62] compared to that of a 0.04 N/m [63] surface stress for the latter one, upon exposure to a 20 mM glucose solution. Similar results have been observed for the detection of H_2O_2[64] and organophosphates.[65]

A2.4 Polymer brushes—Polymer brushes are composed of polymer chains, all approximately the same length, each attached by one end to a solid surface. When bathed in any liquid medium that is a good solvent, the polymer chains stretch away from the surface. Zhou et al. [66] reported that microcantilevers modified by a 20-nm-thick polymethacryloyl ethylene phosphate polymer brush showed a 3.0 N/m surface stress when the pH changed from 6 to 9 or when exposed to a 0.1 M KCl solution (Figure 5). They also observed[67] a 1.0 N/m surface stress on the cantilever surface when applying an alternating positive (0.5 V) and negative (-0.5V) bias to a polyelectrolyte brush-covered cantilever.

A3. Absorption of gas by metal or metal oxide films

Metals or metal oxides with gas-absorption capabilities have been used to modify microcantilevers for gas detection. Because a metal film is thick compared to a monolayer film, absorption of the gases causes a large surface stress on the cantilever.[68] In general, within a certain range, the thicker the film, the greater the bending amplitude. Specific examples include the detection of hydrogen[69,70] and moisture vapor.[71,72]

A4. Phase change of films on the cantilever surface

Phase changing materials are characterized by large changes in volume, which is expected to generate significant surface stress. Guo et al[73] observed more than 5.6 N/m of surface stress on a 10 nm-thick $Ge_2Sb_2Te_5$ (GST) GST film changing from an amorphous state to a crystalline state. Using a thin dielectric capping layer leads to a further increase in surface stress compared to uncapped films.

A5. Surface stress caused by significant intermolecular interactions from adsorbed species

It is now understood that the larger the intermolecular interactions, such as static repulsion, from species on the surface, the larger the surface stress that is generated on the surface.

A5.1. Repulsion by adsorbed molecules on a gold surface—Absorption of a monolayer of thiol compounds on a gold surface caused compressive surface stress that are greater than 0.1 N/m. (Figure 6).[74, 75, 76] This was attributed to apparent dipole moment repulsion from the alkyl chains. Adsorption of a thiol with a single strand of DNA also generated more than 1.0 N/m of surface stress.[77]

A5.2. Surface stress from adsorption of large species on the surface—Adsorption of large molecules or species, such as proteins, on the surface and the subsequent conformational changes of the molecules and/or the interactions of these species could cause a surface stress that is greater than 0.1 N/m. Examples of such large molecules include immoglobulin G and albumin,[78] a lipid vesicle,[79] amyloid,[80] a yeast cell lysate, an antibody, [81] and a phospholipid bilayer.[82]

A5.3. Adsorption of large species on antibody modified microcantilevers—Antibodies provide for chemical specificity. For antibody-based microcantilever sensors, the primary cause of surface stress is the repulsion of target species that are adsorbed onto the antibody film. For this reason, large surface stress changes were observed only for certain large species, such as a GCN4 protein (0.13 N/m),[83] feline coronavirus (0.25 N/m),[84] tularemia (1.74 N/m),[85] E. coli (0.33 N/m),[86] and the anti-myc-tag antibody (0.14 N/m).[87] For cantilevers modified by antibodies for the recognition of small molecules, the surface stress upon adsorption is small, such as the surface stress measured for dichlorodiphenyltrichloroethane (DDT), which was only 0.008 N/m.[88]

However, in some cases, smaller surface stresses were observed when antibody or protein-modified microcantilevers were exposed to the larger species, such as prostate-specific antigen (0.06 N/m)[89] and bacillus subtillis spores (0.01 N/m).[90] This may be due to poor surface coverage by the antibodies. The importance of the surface chemistries will be discussed in section B.

Section B. The strategies to increase surface stress for those conditions under which a large surface stress can not readily be reached

One example in this category is the DNA hybridization on microcantilevers. So far, all of the DNA hybridizations have resulted in surface stresses less than 0.1 N/m,[91] which inhibit the microcantilever sensors from being a viable technology for practical applications. It is often assumed that surface conjugation chemistries utilized by other chip-based microsensors can be transferred to microcantilever devices; however, the mechanism of surface stress induced bending is substantially different from the mechanisms of other sensor platforms such as fluorescence or surface plasmon resonance. Simulation and modeling experiments predict theoretical surface stress on microcantilevers that are much more than the experimentally determined values.[92] Much of the gap between actual and theoretical values is likely due to

non-ideal surface characteristics, including gold surface characteristics, surface packing, orientation of the receptor on the surface, the degree of interaction between the receptors on the surface, changes in receptor conformation and receptor-analyte interactions, etc. Surface packing and orientation can be altered with different surface characteristics and conjugation chemistries. Orientation and surface packing will also affect molecular interactions on the surface. If there is special treatment of the surface and the receptor layer is perfectly immobilized on the surface with both high density and order, the surface stress generated will be in better agreement with the simulated data, thus producing larger bending responses.

This section of the review will summarize our understanding of conjugation chemistry and its relationship to microcantilever responses.

B1. Self-assembled monolayers for the detection of metal ions and small molecules

Functionalizing monolayers was one of the first surface modification approaches developed for microcantilever sensors. Differential surface stress between the two surfaces of a microcantilever is usually accomplished by previous deposition of a thin gold film on one surface of the microcantilever. The gold surface can be selectively functionalized by adsorption of a SAM of thiol compounds.

On clean and smooth surfaces, the origin of the surface stress arises from charge redistribution between the surface and the adsorbates, and from interactions between neighboring surface atoms or molecules with those from the environment. For detecting small molecules or ions, a compact, high density monolayer is the key for obtaining significant binding-induced surfaces stresses. The lateral interaction between adsorbed molecules plays an important role in causing adsorption-driven surface stress, particularly at high coverage. Most of the following approaches to enhance surface stress are based on developing chemistries that achieve a tightly packed, ordered array of receptors on the surface that are sensitive to any slight changes in analyte interaction.

B1.1. Effect of monolayer formation time on sensitivity—Ji, et al. developed[93] a triethyl-12-mercaptododecylammonium (TMA) monolayer modified microcantilever sensor for CrO_4^{2-} detection. It was found that a period of six days is needed to develop a compact monolayer of TMA on a gold surface due to repulsion of the positively-charged ammonium groups in TMA, which contribute to a 0.39 N/m of surface stress upon exposure to a 10^{-3} M of CrO_4^{2-} solution.

B1.2. Photochemical hydrosilylation method—Boiadjiev et al. [94] applied a photochemical hydrosilylation approach to modify the silicon surface of a microcantilever for detection of Cr(VI). Using this method, they achieved a compact surface and the surface stress change was 0.33 N/m when it was exposed to 0.1 mM of Cr(VI).

B1.3. Co-adsorption of long-chain thiols to increase the surface density—A calixcrown molecule, MCC,[95] was anchored onto the gold surface of a microcantilever for Cs^+ detection. When the microcantilever was modified by pure MCC, it did not respond to Cs^+; however, when decane-1-thiol was co-adsorbed at a 2:1 (decane-1-thiol:MCC) ratio to fill the gaps between the two alkyl thiol arms of MCC and the adjacent molecules, a 0.28 N/m surface stress was observed upon exposure to 1 mM of Cs^+. Alvarez et al.[96] also reported the co-adsorption of a thiol compound to form a dense monolayer which enhanced the accessibility of the DNA probes to the target. In this treatment, the thiol compound displaces the weaker adsorptive contacts between the nucleotide chain and gold, covalently attaching to the interstitial regions between chains of ssDNA. The post-treatment ensures that the DNA

probes are only attached to the gold surface through the terminal sulfur atom of the thiol linker attached to the DNA.

B2. Conjugation chemistry selection and different surface morphology

B2.1. The selection of conjugation chemistry and receptors—It has been observed that microcantilevers modified using conjugation chemistries respond differently to the same analytes. In one example,[84] microcantilevers modified by anti-feline infectious peritonitis (FIP) antibody using succinic anhydride did not yield reproducible results for feline coronavirus detection. The poor quality of these cantilevers was determined to be caused by inconsistent surface modification. The consistency and the surface stress were greatly improved when the surface was prepared with 1-ethyl-3-(3-dimethylaminopropyl) carbodimide hydrochloride (EDC) and N-hydroxysuccinimide (NHS). The surface stress was dependant on the active site and the molecular size of the cross-linked compound,[97, 98] and the surface structure and/or the chemistry.[99]

B2.2. Cleanliness of the microcantilever surface—It is commonly accepted that it is essential to clean the surfaces of microcantilevers or employ freshly evaporated and/or electrochemically cleaned surfaces for meaningful results.[100] Besides the gold or silicon surfaces, cleanliness on modified surfaces is also critical for the performance of microcantilever sensors. Unwanted aggregating particles can form on the amino and carboxyl topped thiol monolayers on the gold surfaces. The particles will inhibit crosslinking of EDC/NHS, which may cause unsuccessful microcantilever sensor development. A modified approach utilizing the coexistence of CF_3COOH with the thiols during the SAM process forms a smoother and cleaner surface.[101]

B3. Porous or nanostructured surface

The results from Section A indicate that introducing a thicker layer of receptors or exposing a larger surface area of the microcantilever may enhance the bending amplitude. It is expected that an increased surface area produces a larger number of binding sites and confinement of the molecules in nanocavities, increasing the intermolecular forces such as the solvation, steric, osmotic, and hydration forces with respect to flat surfaces. On the other hand, discontinuities in the gold surface prevents the generated surface stress from being efficiently transferred to the cantilever beam. As a result, reports on this issue from different labs were not consistent, as some reports supported this hypothesis, [102, 103, 104, 105] while others[100, 106,107, 108,109] showed that processed porous silicon surfaces or rough surfaces do not introduce significant static bending of the cantilevers. The poor reproducibility of these studies between different laboratories may be due to differences in the surface properties and the chemistries, such as the degree of roughness or the pore size. In particular, the role of the gold film has not been paid much attention until recently, a topic which will be discussed in the next subsection. A better understanding of the parameters that determine the nature and magnitude of the interaction-driven surface stress needs to be developed in order for microcantilever-based surface stress sensing to become a viable technology.

B4. The effect of the morphology of the gold surface

It was recently realized that the characteristics of the gold surface play a critical role in surface stress optimization, sensitivity, and the reliability of microcantilever sensors. These characteristics include the adhesion[100,110] (so that the surface stress in the sensing film can be transferred to the cantilever substrate), the surface morphology (e.g., grain size, grain boundaries, film roughness, crystallographic orientation, discontinuity), and the cleanliness of the gold sensing surface, which can have both qualitative and quantitative effects on the measured surface stress. It is therefore essential to characterize how these factors affect the

sensor response. Gold surfaces could be prepared using two approaches: thermal evaporation or sputtering. The magnitudes of the surface stresses caused by the same interactions on gold surfaces that are prepared with these two different approaches are significantly different from each other.

B4.1. Thermal evaporation on gold surfaces—Godin et al.[109] showed that the kinetics of SAM formation and the resulting SAM structures are strongly influenced by the surface structure of the underlying gold substrate (Figure 7). Particularly, the adsorption onto gold surfaces having large, flat grains produces high-quality SAMs. An induced compressive surface stress of 15.9 ±0.6 N/m results when a c(4×2) dodecanethiol SAM forms on gold. However, the SAMs formed on small-grained gold (with grain sizes smaller than 100 nm) are incomplete and have an induced surface stress of only 0.51±0.02 N/m. The progression to a fully formed SAM with alkyl chains adopting a vertical (standing-up) orientation is clearly inhibited in the case of small-grained gold substrates and is promoted in the case of large-grained gold substrates.

Tabard-Cossa et al.[100] showed the same results on the adsorption of the thiol molecules, but added that the parameters such as grain size, film roughness, and grain boundaries did not strongly influence the induced surface stress for anion adsorption and the surface stress response is more dependent on the continuity of the gold sensing surface than on its average grain size.

B4.2. Sputter coated gold surface—Kadam et al.[111] studied the Hg sensing behavior of microcantilevers that were modified with as-deposited sputtered and thermally evaporated Au film. For sputtered films, the deflection response of the microcantilever always stabilizes after the Hg is turned off, whereas for thermally evaporated films there is an exponential decay after the Hg exposure is stopped. It should be noted that this is only for Hg detection. No such comparison has been made for detection of alkylthiols or biomolecules.

Merten et al.[112] found that the higher the growth rate of the gold layer, the smaller the surface stress, because higher growth rates of the gold film produce a higher degree of coalescence (Figure 8). Microcantilevers in which the gold coating has not undergone coalescence are characterized by large values of tensile stress of about 2.3–2.6 N/m (to mecaptohexanol). The surface stress was also related to the thickness of the sputtered gold film. Two relative maxima of surface stress to adsorption can be found when the thickness of the gold films is 20 nm or 60 nm. In these films, there is a high elastic strain energy accumulated in the nanoislands that is partially relieved by the attachment of the mecaptohexanol molecules. They also found that there is not a ready relationship between the adsorption surface stress and the roughness of the gold film, i.e. the gold nanostructure does not play a fundamental role in the surface stress that is induced by alkylthiol adsorption.

Perspective on microcantilever sensing

Microcantilever sensor technology has been steadily growing for the past fifteen years. However, there is still a long way to go before these surface-stress-based sensors can be applied to industry, with biosensing lacking in particular, which is mainly because of low signal/noise (S/N) ratios.

The ideal and direct sensing mechanism involves measuring either the binding-reduced bending or the surface stress change on the micocantilevers. To achieve a fast response, the preferred surface modification approach for sensing involves conjugating an ultrathin layer of receptors on the surface of the microcantilevers. However, the reported surface stresses of these sensors are in general quite small, due to both the poor characteristics of the gold surface and

the surface chemistries, and thus surface modification is critical for developing sensitive and reliable microcantilever sensors. To achieve this goal, a better understanding of the core parameters that determine the magnitude of the interaction-driven surface stress needs to be established in order to improve the sensitivity, stability, and reproducibility of microcantilever sensors. These parameters include:

1. The effects of the morphology and the continuity of the gold surface on the density of the conjugated receptor coating and the subsequent sensing performance need to be well understood.
2. Various factors, such as the selection of conjugation chemistries, the surface chemistry reaction time, and the co-adsorption need to be considered and optimized in order to enhance the packing density of the coatings.
3. Surface cleaning procedures for gold surfaces and chemically functionalized surfaces need to be developed.
4. If the characteristics of the gold surface do not meet the demanding requirements for microcantilever sensing, conjugation chemistries on other surfaces, such as a silicon surface, would be worth investigation in order to develop reliable sensors based on microcantilevers. Few works have been contributed to this field in the past.

After modification, if the above approaches, which are based on either monolayers or ultra thin layers, are indeed not enough to produce both a sufficient surface stress and reproducibility for reliable sensing, surface coatings based on relatively thicker films will need to be used for the direct sensing approach. As shown in section A, numerous cases showed that microcantilevers coated with thicker films generated large bending on sorption analytes. Microcantilevers with thicker coatings do not require a high maintenance of the surface characteristics of microcantilevers, but mainly rely on the properties of the materials of the coating. The materials of these films are mostly polymers, such as hydrogels, polymer brushes, porous polymers, metal organic complexes,[113] etc. Several recent publications[114,115] have shown that microcantilevers modified by these polymers could be quite promising if applied to biosensing. Along this line, it is expected that a film of dentrimers could also provide the solution, although dentrimers have not yet been applied to microcantilevers. The negative consequence of this new polymer film approach is that there would be a longer response time due to the diffusion of the analytes into the film. It should be noted that although all of the thick-film modified microcantilevers showed large bending and were out of the focus of this review, several aspects, such as the viscoelastic effect, of these coatings, should be paid serious attention in order to develop reliable sensors. Even though large bending is a necessity, it does not guarantee reproducible and reliable sensing. This has been discussed in more detail in another review paper.[116]

Besides a thicker film coating, another possibility, based on binding or interaction, could induce a significant change in the substrate, such as collapse, phase change, or polarization change of the substrates. Like the thicker film coating, this also does not require high maintenance of the surface characteristics.

It is noteworthy that several indirect approaches may provide alternate ways to enhance microcantilever bending for reliable sensing. The first is by applying electrochemistry to microcantilevers such as those discussed in section A. Two other examples are:

1. *Compare the characteristics of the surfaces before and after the receptor-analyte interaction*. As an example, traditionally, detection of DNA hybridization is conducted in solution but the surface stress is generally less than 0.1 N/m. An alternative approach is to compare the hydration-induced surface stress of ssDNA with that of hybridized DNA in the gas phase. [117] In this work, Merten et al. showed

that cantilevers modified with ssDNA and hybridized DNA have different surface stress changes that differ by more than 0.1 N/m when they undergo hydration changes at various moistures levels.

2. *Magnetostrictive cantilevers*. This represents an effective approach for the detection of biomolecules by an enhanced amplification of the deflection amplitude (but is not due to surface stress change). The method involves the association of magnetic particles, which carry the biorecognition complex to the functionalized cantilever, with the magneto-mechanical deflection of a cantilever in the presence of an external magnet. It was shown that this magneto-mechanical method could detect trace amounts of extremely dilute biological samples with large bending amplitudes.[118]

Acknowledgments

Dr. Ji would like to thank Majithia Ravish and Chandrakanth Alluri for their efforts in parts of the literature search while he was at Louisiana Tech University. This work was supported by National Institutes of Health (NIH) Grant Number 1R01NS057366. The contents of this paper are solely the responsibility of the authors and do not necessarily represent the official views of the agencies funding this work.

References

1. Gimzewski JK, Gerber C, Meyer E, Schlittler RR. Chem Phys Lett 1994;217:589–594.
2. Chen GY, Warmack RJ, Thundat T, Allison DP, Huang A. Rev Sci Instrum 1994;65:2532–2537.
3. Thundat T, Warmack RJ, Chen GY, Allison DP. Appl Phys Lett 1994;64:2894–2896.
4. Kolesar ES, Allen PB, Howard JT, Wilken JM, Boydston N. Thin Solid Films 1999;355-356:295–302.
5. Thundat T, Sharp SL, Fisher WG, Warmack RJ, Wachter EA. Appl Phys Lett 1995;66:1563–1565.
6. Pan CS, Hsu W. J Microelectromechan Sys 1999;8:200–207.
7. Finot E, Thundat T, Lesniewska E, Goudonnet JP. Ultramicroscopy 2001;86:175–180. [PubMed: 11215621]
8. Raiteri R, Butt HJ. J Phys Chem 1995;99:15728–15732.
9. Davis ZJ, Abadal G, Kuhn O, Hansen O, Grey F, Biosen A. J Vac Sci Technol, B 2000;18:612–616.
10. Boskovic S, Chon JW, Mulvaney P, Sader JE. J Rheology 2002;46:891–899.
11. Bachels T, Schafer R. Rev Sci Instru 1998;69:3794–3797.
12. Yamada H, Itoh H, Watanabe S, Kobayashi K, Matsushige K. Surf Interface Anal 1999;27:503–506.
13. Fritz J, Baller MK, Lang HP, Rothuizen H, Vettiger P, Meyer E, Guntherodt HJ, Gerber Ch, Gimzewski JK. Science 2000;288:316–318. [PubMed: 10764640]
14. Hansen KM, Ji HF, Wu G, Datar R, Cote R, Majumdar A, Thundat T. Anal Chem 2001;73:1567–1571. [PubMed: 11321310]
15. Jensenius H, Thaysen J, Rasmussen AA, Veje LH, Hansen O, Boisen A. App Phys Lett 2000;76:2615–2617.
16. Thundat T, Wachter EA, Sharp SL, Warmack RJ. Appl Phys Lett 1995;66:1695–1697.
17. Wu G, Datar RH, Hansan KM, Thundat T, Cote RJ, Majumdar A. Nature Biotech 2001;19:856–860.
18. Stoney GG. Proc Roy Soc (London) 1909;82:172–175.
19. Wachter EA, Thundat T, Oden PI, Warmack RJ, Datskos PG, Sharp SL. Rev Sci Instrum 1996;67:3434–3439.
20. Pinnaduwage LA, Gehl A, Hedden DL, Muralidharan G, Thundat T, Lareau RT, Sulchek T, Manning L, Rogers B, Jones M, Adams JD. Nature 2003;425:474–474. [PubMed: 14523436]
21. Thundat T, Oden PI, Warmack RJ. Microscale Thermophys Engineering 1997;1:185–199.
22. Ji HF, Zhang Y, Purushotham VV, Kondu S, Ramuchandran B, Thundat T, Haynie DT. Analyst 2005;130:1577–1579. [PubMed: 16284654]
23. Mutyala MSK, Bandhanadham D, Pan L, Pendyala VR, Ji HF. Acta Mechan Sinica 2009;25:1–12.
24. Fritz J. Analyst 2008;133:855–863. [PubMed: 18575634]
25. Finot E, Passian A, Thundat T. Sensors 2008;8:3497–3541.

26. Su M, Dravid V. Nano Lett 2005;5:2023–2028. [PubMed: 16218731]
27. Fang W, Tsai HC, Lo CY. Sens Actuat A 1999;77:21–27.
28. Lin YH, McConney ME, LeMieux MC, Peleshanko S, Jiang C, Singamaneni S, Tsukruk VV. Adv Mater 2006;18:1157–1161.
29. Thundat T, Finot E, Hu Z, Ritchie RH, Wu G, Majumdar A. Appl Phys Lett 2000;77:4061–4063.
30. Kadam AR, Nordin GP, George MA. J Appl Phys 2006;99:904–905.
31. Xu X, Thundat T, Brown GM, Ji HF. Anal Chem 2002;74:3611–3615. [PubMed: 12175144]
32. Cherian S, Mehta A, Thundat T. Langmuir 2002;18:6935–6939.
33. Butt HJ. J Coll Interface Sci 1996;180:251–260.
34. Cherian S, Thundat T. Appl Phys Lett 2002;80:2219–2221.
35. Pinnaduwage LA, Hawk JE, Boiadjiev V, Yi D, Thundat T. Langmuir 2003;19:7841–7844.
36. Raiteri R, Butt HJ, Grattarola M. Electrochem Acta 2000;46:157–163.
37. Brunt TA, Rayment, O'Shea SJ, Welland ME. Langmuir 1996;12:5942–5946.
38. Tabard-Crossa V, Godin M, Beaulieu LY, Grutter P. Sens Actuat B 2005;107:233–241.
39. Tian F, Boiadjiev VI, Pinnaduwage LA, Brown GM, Thundat T. J Vac Sci Technol A 2005;23:1022–1028.
40. Quist F, Tabard-Cossa V, Badia A. J Phys Chem B 2003;107:10691–10695.
41. Norman L, Badia A. J Amer Chem Soc 2009;131:2328–2337. [PubMed: 19166296]
42. Juluri BK, Kumar AS, Liu Y, Ye T, Yang YW, Flood AH, Fang L, Stoddart JF, Weiss PS, Huang TJ. ACS NANO 2009;3:291–300. [PubMed: 19236063]
43. Lahav M, Durkan C, Gabai R, Katz E, Willner I, Welland ME. Angew Chem Int Ed 2001;40:4095–4097.Note: the reported surface stress might be calculated incorrectly using data from this paper. The authors stated “the deflection by 1 nm corresponds to a surface stress of 1.7 N/m”. From our calculations, 1 nm deflection of cantilevers by the authors should correspond to a surface stress of 1.8 mN/m.
44. Tabard-Cossa V, Godin M, Grutter P. J Phys Chem B 2005;109:17531–17537. [PubMed: 16853242]
45. Battiston FM, Ramseyer JP, Lang HP, Baller MK, Gerber Ch, Gimzewski JK, Meyer E, Guntherodt HJ. Sens Actuat B 2001;77:123–131.
46. Arora WJ, Tenhaeff WE, Gleason KK, Barbastathis G. J Microelectromech Sys 2009;18:97–102.
47. Lang HP, Baller MK, Berger R, Gerber Ch, Gimzewski JK, Battiston FM, Fornaro P, Ramseyer JP, Meyer E, Guntherodt HJ. Anal Chim Acta 1999;393:59–65.
48. Lang HP, Berger R, Battiston F, Ramseyer JP, Meyer E, Andreoli C, Brugger J, Yettiger P, Despont M, Mezzacasa T, Scandella L, Guntherodt HJ, Gerber Ch, Gimzewski JK. Appl Phys A 1998;66:S61–S64.
49. Jensenius H, Thaysen J, Rasmussen AA, Veje LH, Hansen O, Boisen A. Appl Phys Lett 2000;76:2615–2617.
50. Wright YJ, Kar AK, Kim YW, Scholz C, George MA. Sens Actuat B 2005;107:242–251.
51. Battiston FM, Ramseyer JP, Lang HP, Baller MK, Gerber Ch, Gimzewski JK, Meyer E, Guntherodt HJ. Sens Actuat B 2001;77:122–131.
52. Betts TA, Tipple CT, Sepaniak MJ, Datskos PG. Anal Chim Acta 2000;422:89–99.
53. Thundat T, Chen GY, Warmack RJ, Allison DP, Wachter EA. Anal Chem 1995;67:519–521.
54. Cherian S, Gupta RK, Mullin BC, Thundat T. Biosen Bioelectro 2003;19:411–416.
55. Lemieux MC, McConney ME, Lin YH, Singamaneni S, Jiang H, Bunning TJ, Tsukruk VV. Nano Lett 2006;6:730–734. [PubMed: 16608273]
56. Bashir R, Hilt JZ, Elibol O, Gupta A, Peppas NA. Appl Phys Lett 2002;81:3091–3093.
57. Ji HF, Yan X, Mcshane MJ. Diab Tech Therap 2005;7:986–995.
58. Zhang Y, Ji HF, Brown G, Thundat T. Anal Chem 2003;75:4773–4777. [PubMed: 14674453]
59. Liu K, Ji HF. Anal Sci 2004;20:9–11. [PubMed: 14753251]
60. Mao JS, Kondu S, Ji HF, McShane MJ. Biotechnology and Bioengineering 2006;95:333–341. [PubMed: 16894636]

61. Valiaev A, Abu-Lail NI, Lim DW, Chilkoti A, Zauscher S. Langmuir 2007;23:339–344. [PubMed: 17190524]
62. Yan X, Xu XK, Ji HF. Anal Chem 2005;77:6197–6204. [PubMed: 16194079]
63. Subramanian A, Oden PI, Kennel SJ, Jacobson KB. Appl Phys Lett 2002;81:385–387.
64. Yan X, Shi X, Hill K, Ji HF. Anal Sci 2006;22:205–208. [PubMed: 16512409]
65. Karnati C, Du H, Ji HF, Xu X, Lvov Y, Chen W, Mulchandani A. Biosensor Bioelectronics 2007;22:2636–2642.
66. Zhou F, Shu W, Welland ME, Huck WTS. J Amer Chem Soc 2006;128:5326–5327. [PubMed: 16620088]
67. Zhou F, Biesheuvel M, Choi EY, Shu W, Poetes R, Steiner U, Huck WTS. Nano Lett 2008;8:725–730. [PubMed: 18269260]
68. Lang HP, Berger R, Andreoli C, Brugger J, Despont M, Vettiger P, Gerber Ch, Gimzewski JK. Appl Phys Lett 1998;72:383–385.
69. Hu Z, Thundat T, Warmack RJ. J Appl Phys 2001;90:427–431.
70. Chou YI, Chiang HC, Wang CC. Sens Actuat 2008;129:72–78.
71. Kapa P, Liu P, Chen Q, Morishetti D, Mutyala MS, Fang J, Varahramyan K, Ji HF. Sen Actuat B Chem 2008;134:390–395.
72. Lee D, Shin N, Lee KH, Jeon S. Sens Actuat B Chem 2009;137:561–565.
73. Guo Q, Li M, Li Y, Shi L, Chong TC, Kalb JA, Thompson CV. Appl Phys Lett 2008;93:221907.
74. Berger R, Delamarche E, Lang HP, Gerber C, Gimzewski JK, Meyer E, Guntherodt HJ. Science 1997;276:2021–2024.
75. Mertens J, Alvarez M, Tamayo J. Appl Phys Lett 2005;87:234102.
76. Datskos PG, Sauers I. Sens Actuat 1999;61:75–82.
77. Marie R, Jensenius H, Thaysen J, Christensen CB, Biosen A. Ultramicroscopy 2002;91:29–36. [PubMed: 12211481]
78. Moulin AM, O'Shea SJ, Badley RA, Doyle P, Welland ME. Langmuir 1999;15:8776–8779.
79. Ghatkersar MK, Lang HP, Gerber C, Hegner M, Braun T. PLoS One 2008;3:e3610. [PubMed: 18978938]
80. Knowles TP, Shu W, Huber F, Lang HP, Gerber C, Dobson CM, Welland ME. Nanotech 2008;19:384007.
81. Shu W, Laurenson S, Knowles TPJ, Ferrigno PK, Seshia AA. Biosens Bioelectro 2008;24:233–237.
82. Pera I, Fritz J. Langmuir 2007;23:1543–1547. [PubMed: 17241085]
83. Backmann N, Zahnd C, Huber F, Bietsch A, Pluckthun A, Lang HP, Guntherodt HJ, Hegner M, Gerber C. PNAS 2005;102:14587–14592. [PubMed: 16192357] The author provided a thickness of 0.5 μm, but no information on the length. The 0.13 N/m surface stress was calculated assuming that the length of the cantilever was 500 μm, which was a standard length of cantilevers fabricated by the IBM Zurich Research Laboratory.
84. Velanki S, Ji HF. Meas Sci Technol 2006;17:2964–2968.
85. Yan X, Zhang J, Ji HF, Thundat T. Expert Review of Molecular Diagnostics 2004;4(6):859–866. [PubMed: 15525227]
86. Zhang J, Ji HF. Anal Sci 2004;20:585–587. [PubMed: 15116951]
87. Kim BH, Mader O, Weimar U, Brock R, Kern DP. J Vac Sci Technol B 2003;21:1472–1475.
88. Alvarez M, Calle A, Tamayo J, Lechuga LM, Abad A, Montoya A. Biosens Bioelectro 2003;18:649–653.
89. Wu G, Datar RH, Hansen KM, Thundat T, Cote RJ, Majumdar A. Nature Biotech 2001;19:856–860.
90. Dhayal B, Henne WA, Doorneweerd DD, Reifenberger RG, Low PS. J Amer Chem Soc 2006;128:3716–3721. [PubMed: 16536545]
91. Yan X, Ji HF, Thundat T. Curr Anal Chem 2006;2:297–307.
92. Liu F, Zhang Y, Ou-Yang Z. Biosens Bioelectron 2003;18:655–660. [PubMed: 12706575]
93. Ji HF, Thundat T, Dabestani R, Brown GM, Britt PF, Bonnesson P. Anal Chem 2001;73:1572–1576. [PubMed: 11321311]

94. Boiadjieve VI, Brown GM, Pinnaduwage LA, Goretzki G, Bonnesen PV, Thundat T. Langmuir 2005;21:1139–1142. [PubMed: 15697249]
95. Ji HF, Dabestani R, Finot E, Thundat T, Brown GM, Britt PF. Chem Commun 2000:457–458.
96. Álvarez M, Carrascosa LG, Moreno M, Calle A, Zaballos Á, Lechuga LM, Martinez-A C, Tamayo J. Langmuir 2004;20:9663–9668. [PubMed: 15491200]
97. Kim DJ, Weeks BL, Hope-Weeks LJ. Scanning 2007;29:245–248. [PubMed: 18076074]
98. Lai SM, Wu CY, Hsu KS, Wang CC, Chiang HC, Lu KL, Chou YI. Electrochem Solid State Lett 2007;10:J161–J164.
99. Shu W, Laue ED, Seshia AA. Biosens Bioelectro 2007;22:2003–2009.
100. Tabard-Cossa V, Godin M, Burgess IJ, Monga T, Lennox RB, Grutter P. Anal Chem 2007;79:8136–8143. [PubMed: 17914755]
101. Gao H, Buchapudi KR, Harms-Smyth A, Schulte MK, Xu X, Ji HF. Langmuir 2008;24:345–349. [PubMed: 18154314]
102. Tipple CA, Lavrik NV, Culha M, Headrick J, Datskos P, Sepaniak MJ. Anal Chem 2002;74:3118–3126. [PubMed: 12141672]
103. Lavrik NV, Tipple CA, Sepaniak MJ, Datskos PG. Biomed Microdev 2001;3:35–44.
104. Lavrik NV, Tipple CA, Sepaniak MJ, Datskos PG. Chem Phys Lett 2001;336:371–376.
105. Headrick JJ, Sepaniak MJ, Lavrik NV, Datskos PG. Ultramicroscopy 2003;97:417–424. [PubMed: 12801697]
106. Stolyarova S, Cherian S, Raiteri R, Zeravik J, Skladal P, Nemirovsky Y. Sens Actuat B 2008;131:509–515.
107. Lee D, Kim EH, Yoo M, Jung N, Lee KH, Jeon S. Appl Phys Lett 2007;90:113107.
108. Desikan R, Lee I, Thundat T. Ultramicroscopy 2006;106:795–799. [PubMed: 16678968]
109. Godin M, Williams PJ, Cossa VT. Langmuir 2004;20:7090–7096. [PubMed: 15301492]
110. Haiss W. Rep Prog Phys 2001;64:591–648.
111. Kadam AR, Nordin GP, George MA. J Vac Sci Technol B 2006;24:2271–2275.
112. Mertens J, Calleja M, Ramos D, Taryn A, Tamayo J. J Appl Phys 2007;101:034904.
113. Allendorf MD, Houk RJT, Andruszkiewicz L, Talin AA, Pikarsky J, Choudhury A, Gall KA, Hesketh PJ. J Amer Chem Soc 2008;130:14404–14405. [PubMed: 18841964]
114. Koev ST, Powers MA, Yi H, Wu LQ, Bentley WE, Rubloff GW, Payne GF, Ghodssi R. Lab Chip 2007;7:103–111. [PubMed: 17180212]
115. Chen, T.; Desikan, R.; Datar, R.; Zauscher, S. Inter. Workshop on Nanomech. Cant Sensors; 2008, May 19-21;
116. Goeders KM, Colton JS, Bottomley LA. Chem Rev 2008;108:522–542. [PubMed: 18229951]
117. Mertens J, Rogero C, Calleja M, Ramos D, Martin-Gago JA, Briones C, Tamayo J. Nature Nanotech 2008;3:301–307.
118. Weizmann Y, Patolsky F, Lioubashevski O, Willner I. J Am Chem Soc 2004;126:1073. [PubMed: 14746475]

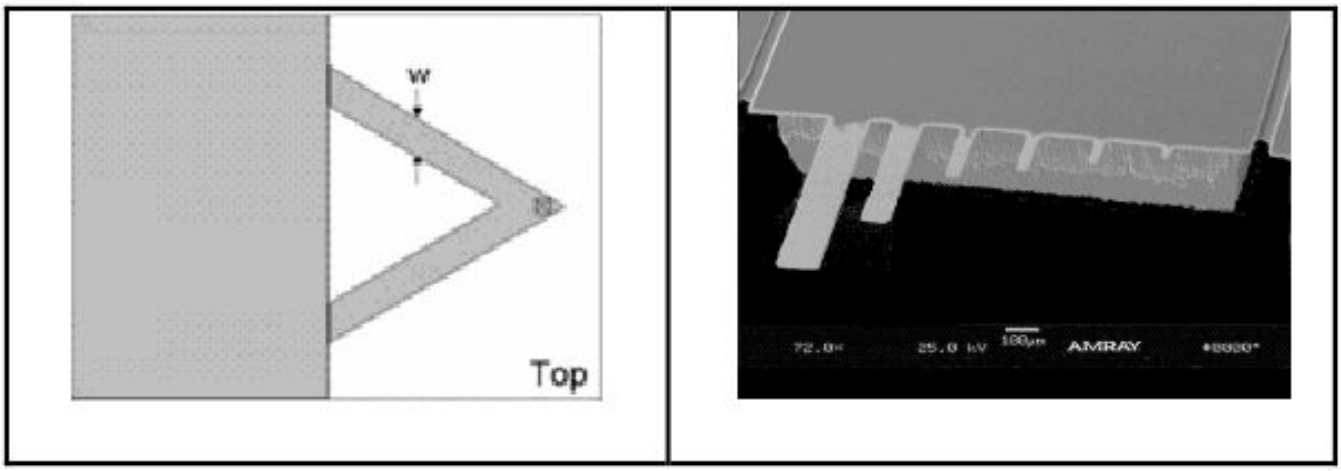

Figure 1.
Scheme (left, Veeco Instruments, Santa Barbara, CA) and Electron micrograph (right, fabricated in our lab) of cantilevers. The sizes of the cantilevers on the right vary from 5 μm to 200 μm in length, extending from the support.

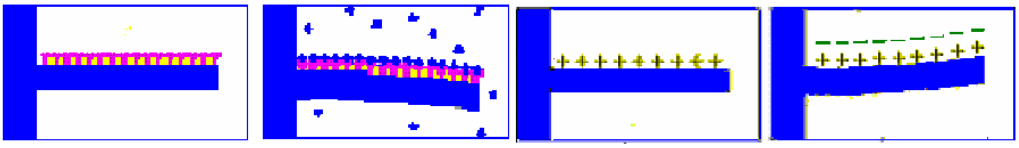

Figure 2.
Two mechanisms of binding-induced surface stress on different types of responsive coatings. Left: tensile stresses for antigen-antibody interaction; right: compressive stress due to neutralization of excessive charge on the surface.

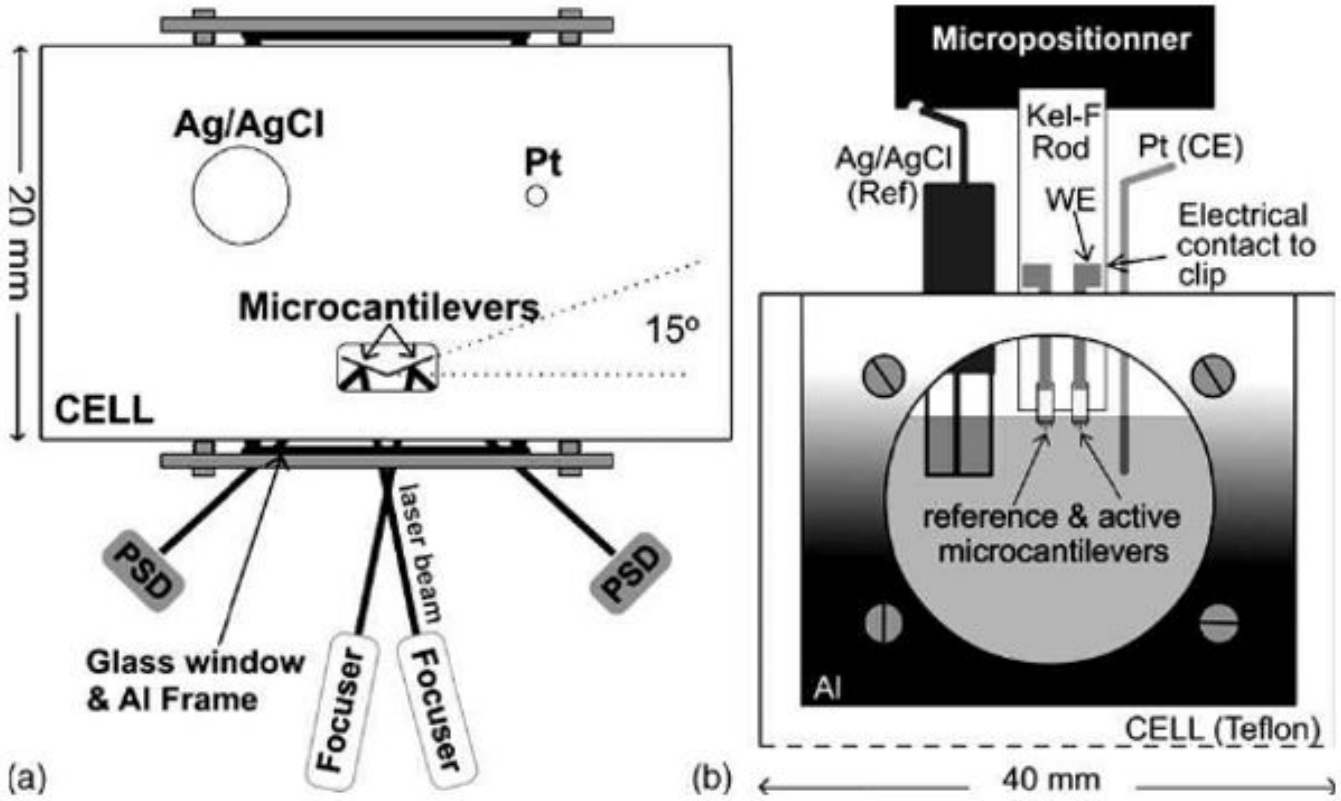

Figure 3.
(a) Top view of the system. A schematic representation of the front of the cell is shown in (b). Reprinted with permission from the Elsevier B.V.

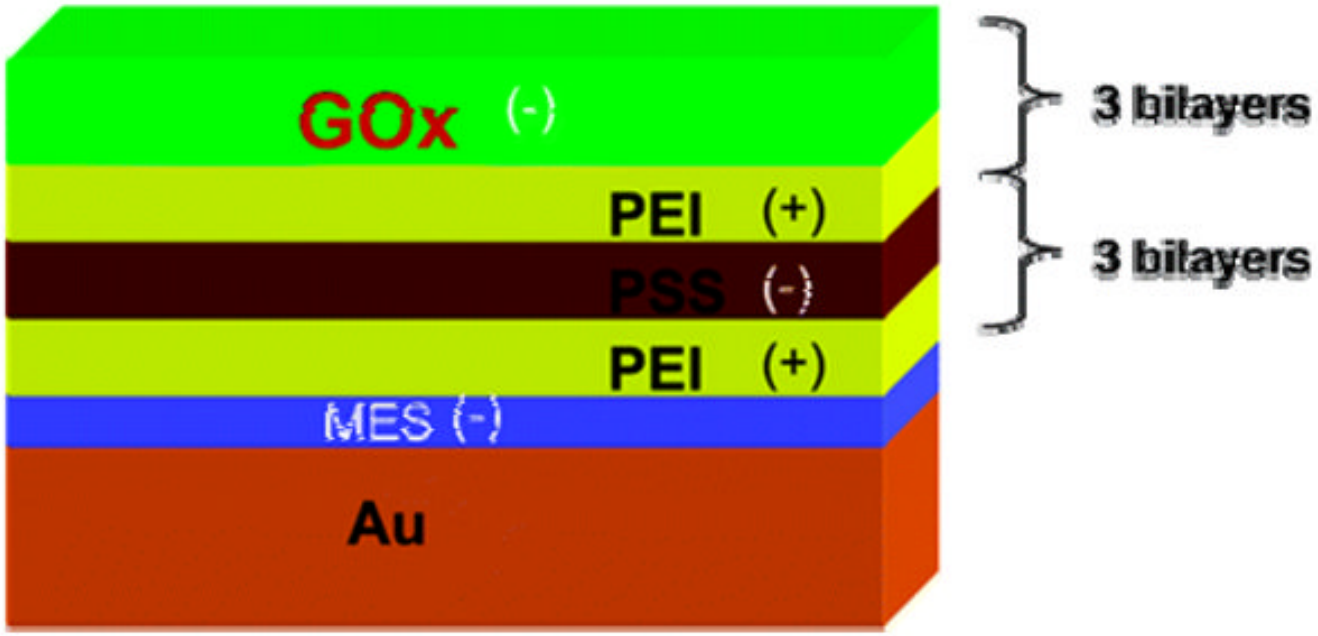

Figure 4.
LbL nanoassembly with intercalated enzyme on the MCL surface. Reprinted with permission from the American Chemical Society.

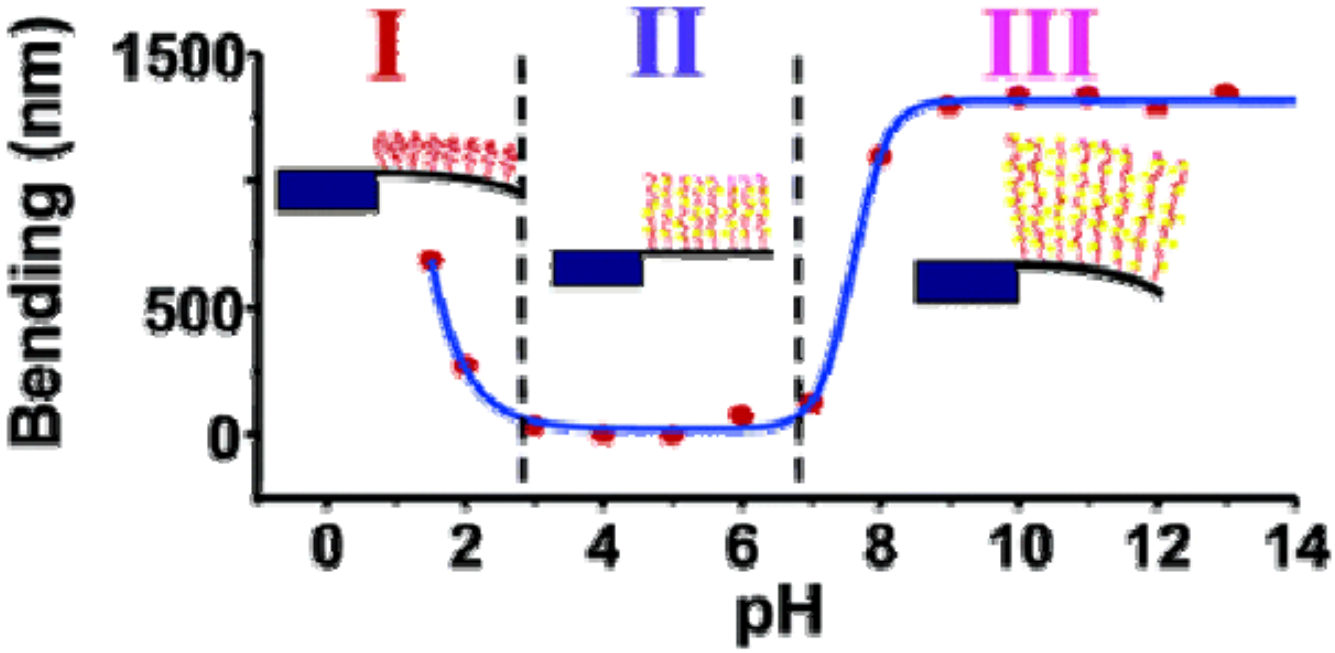

Figure 5.
Bending of single-side brush-modified cantilever with changing pH and schematic illustration of brush conformation in different regimes. Reprinted with permission from the American Chemical Society.

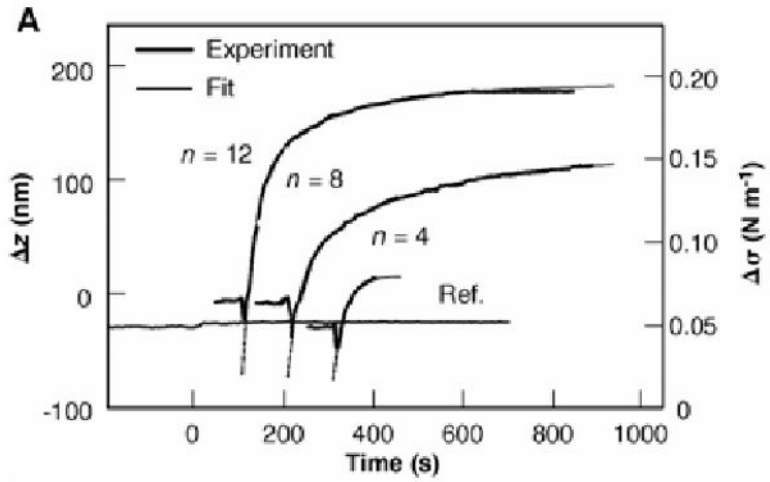

Figure 6.
Deflection, Δz, and changes in surface stress, Δσ, of the sensors are plotted as a function of time for exposure to alkanethiol and a reference vapor. Reprinted with permission from the American Association for the Advancement of Science.

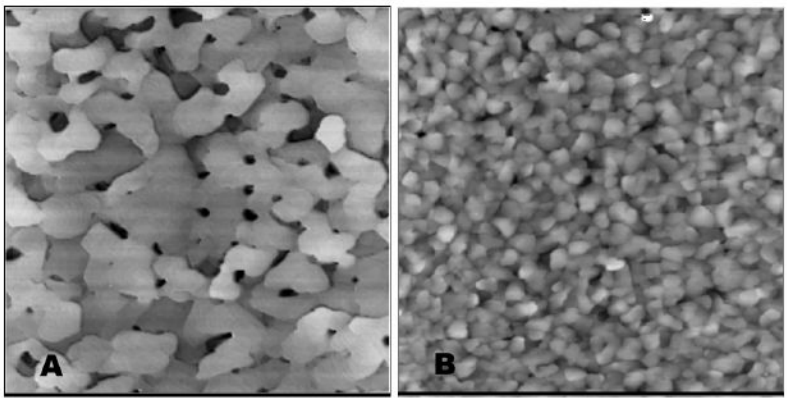

Figure 7.
STM images (3 μm × 3 μm) of (A) large-grained gold and (B) small-grained gold. Reprinted with permission from the American Chemical Society.

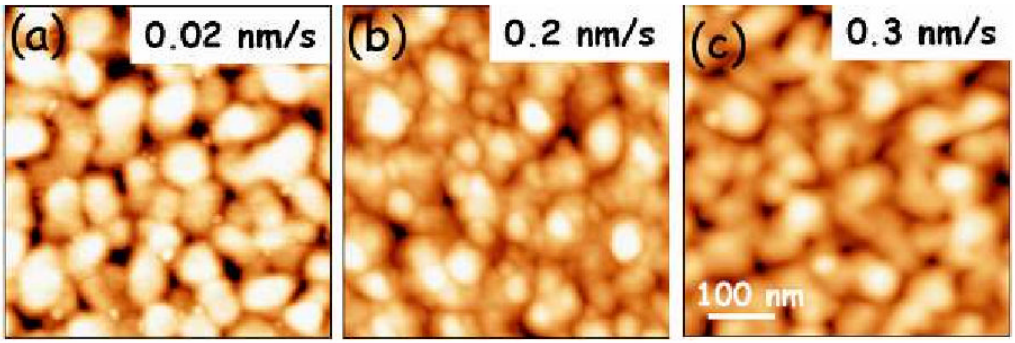

Figure 8.
Atomic force microscopy topography images ($0.5 \times 0.5\ \mu m^2$) of 60 nm thick gold films deposited on the silicon cantilevers at (a) 0.02 nm/s, (b) 0.2 nm/s, and (c) 0.3 nm/s. Reprinted with permission from the American Institute of Physics.

Table 1

Surface stress of polymer coated microcantilevers caused by absorption of the gas molecules

Electrochemical process	Surface stress
Deposition and stripping of Pb (Figure 5) on Au(111) surface[37]	1.0 N/m
Electrochemical adsorption of ClO_4^- on the gold-coated surface[38]	1.28 ±0.13 N/m
Redox of Cr(VI) ions[39]	2.5 N/m per volt
Oxidation of the surface-bound ferrocene[40,41]	-0.20±0.04 N/m
redox-controllable, bistable [3] rotaxane molecules [42]	0.13 N/m

Table 2
Polymer coated microcantilevers for the detection of chemicals

Polymers	Thickness	Sensing analyte
Polymethylmethacrylate[47,48]	N/A	Butanol and methanol
AZ 5200 photoresist polymer[49]	N/A	
Polyethylene glycol[50]	N/A	
Polyvinylchloride[51]	N/A	ethanol
A polymeric chromatographic stationary phase, SP-2340[52]	50-500 nm	ethanol or methylene chloride
Gelatin[53]	23 nm	moistures